On protein quality control, myofibrillar myopathies, and neurodegeneration

Meister, Melanie

CHAPTER 4

DNAJB6 delays Neurodegeneration in a *Drosophila melanogaster* Model for Huntington's Disease via Non-Cell Autonomous Mechanisms

Matteo Bason, Melanie Meister-Broekema, Niels Alberts, Pascale Dijkers, Steven Bergink, Ody Sibon, Harm H. Kampinga

Department of Cell Biology, University of Groningen, University Medical Center Groningen, Groningen, The Netherlands

Abstract

Heat Shock Proteins (HSPs) are key regulators in cellular protein quality control (PQC) and have been suggested to play an essential role in protecting cells against protein aggregate-related neurodegenerative diseases.[1] Astrocytic changes, including progressive molecular, cellular, and functional changes are common hallmarks in these diseases and thought to be aimed at counteracting the progression of neurodegeneration.[2] The magnitude of this response tends to depend on the severity of the insult. More and more evidence is accumulating indicating that HSPs are part of this astrocytic response to neurodegenerative diseases as well. However, it is yet unknown whether and how elevated astrocytic expression of specific HSPs may confer *in vivo* protection against neuronal degeneration. In Huntington's disease (HD), expansions of the polyglutamine (polyQ) tract facilitates the aggregation of Huntingtin (Htt), which drives cell degeneration, particularly in the striatal medium spiny neurons, and has a central role in disease pathogenesis. DNAJB6 is a human HSP of the DNAJ family and was identified to be the most potent suppressor of PolyQHtt-aggregation.[3,4] Here we show that the exclusively astrocytic DNAJB6-overexpression extends lifespan and delays neurodegeneration in a pan-neuronal HttPolyQ-*Drosophila melanogaster* model, thus providing evidence for a non-cell autonomous protective role of astrocytes expressing specific HSPs in HD.

Our laboratory has previously identified DNAJB6, a human HSP of the DNAJ family and HSP70 co-chaperone, as possessing potent anti-polyQ aggregation properties *in vitro* and *in vivo.*[3,4] To verify whether the protective effects of DNAJB6 are conserved in *D. melanogaster*, we co-expressed human HttQ100-mRFP[5], human DNAJB6[6], and the membrane-targeted fluorescent reporter mCD8-GFP[7] in *D. melanogaster* ommatidiam, which is a structure of the compound eyes containing photoreceptors and support cells, using the GMR promoter driven by the Gal4-UAS expression system.[8] Our experiments confirmed DNAJB6-co-expression resulted in a significant alleviation of HttQ100-mRFP-associated increase in mCD8-GFP fluorescence in ommatidia and total mCD8-GFP protein levels (Fig.1A, 1B, S1A, S1B). Taken together with our results indicating that co-expression of DNJB6 also reduced the amount of HttQ100-mRFP aggregates in total head lysates (Fig. S1C), these data indicate that the cell-autonomous protective effects of human DNAJB6 against polyQHtt-mediated aggregation are conserved in *D. melanogaster*.

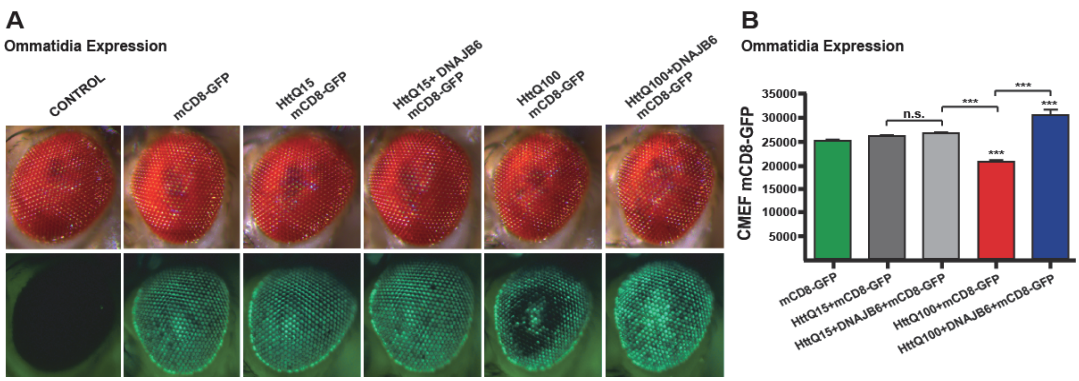

Figure 1: DNAJB6 cell-autonomous protective effects against polyQHtt-mediated cellular degeneration in D. melanogaster ommatidia. A*) Representative images of D. melanogaster eyes (♂, Gal4-UAS system, 48 hours old adults) following GMR-driven expression of indicated transgenes in ommatidia. mCD8-GFP served as a reporter for retinal integrity; genotypes: w(-); UAS Htt (Q15-mRFP or Q100-mRFP) / + (or UAS V5-DNAJB6); GMR Gal4 / UAS mCD8-GFP (or +).* ***B****) Quantification of the corrected mean eye fluorescence (CMEF) for mCD8-GFP. Statistical significance analyzed using 10 eyes/group with 1-way ANOVA test (SEM, ***, p<0,001).*

Next, we generated a *D. melanogaster* line expressing HttQ100-mRFP in all neurons using the pan-neuronal promoter ELAV-Gal4 (Fig S2A).[9] Western blots of total head lysates of *D. melanogaster* expressing HttQ100-mRFP indicate the abundant presence of Htt monomers, cleaved Htt-products, Htt-aggregate intermediates, and high molecular weight (HMW) Htt-aggregates in 5 day-old adult males (Fig. 2A) and females (Fig. S2B). Remarkably, compared to 5-day old *D. melanogaster,* the presence of Htt-monomers and -intermediates species was decreased in 15-day old adults, while HMW Htt-aggregates were still present, indicating a worsening of the HD-phenotype. Lifespan analysis showed a significant reduction in lifespan of HttQ100-mRFP-expressing males (Fig. 2B, S2C) and females (Fig. S2D, S2E), with a T_{50}-decrease of 55% and 62%, respectively. This finding was further supported by a significant decrease in the climbing assay-based fitness score in HttQ100-mRFP males starting at day 12 (Fig. S2F).

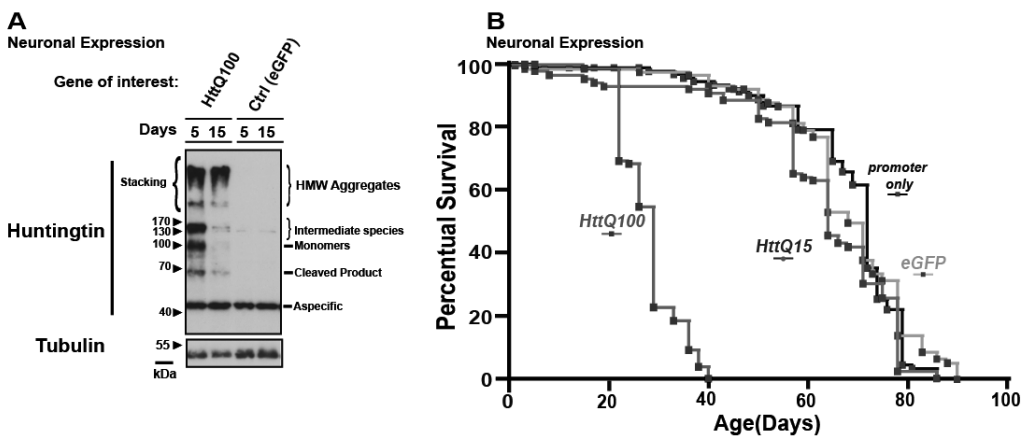

Figure 2: PolyQ-Htt protein levels and survival curve in D. melanogaster following pan-neuronal expression of HttQ100-mRFP. A) *Representative Western blots of total D. melanogaster head lysates (♂, Gal4-UAS system, 5 and 15 days old adults) following targeted pan-neuronal expression of the indicated transgenes. The anti-Htt antibody was used to detect various HttQ100-mRFP-species (100 kDa-monomers, 70kDa-cleaved products, 130-170 kDa-intermediate aggregate species, HMW aggregates in stacking gel), Tubulin was as loading control. Genotypes: w(-); UAS HttQ100-mRFP (or UAS eGFP) / +; ELAV Gal4/+).* ***B)*** *Lifespan of isogenized D. melanogaster lines (♂, Gal4-UAS system) pan-neuronally expressing HttQ100-mRFP or control transgene (HttQ15-mRFP, eGFP or only promoter) inusing ELAV. Statistical significance was analyzed in ≈100 flies/group by the Log rank Mantel-Cox test. Please, refer to S2C for detailed statistics and genotypes.*

To further investigate the cell-autonomous protective effects of DNAJB6 against pan-neuronal polyQHtt-mediated toxicity,[4] we generated *D. melanogaster* lines expressing HttQ100-mRFP via the Gal4-UAS and DNAJB6 via the LexA-LexO expression system.[10] Protein expression was targeted to neurons via the ELAV driver in both systems. The autonomy of the Gal4-UAS and LexA-LexO systems was verified (Fig.S3A, S3B) and two different LexA trans-activator lines were used to control the magnitude of LexO-DNAJB6-expression levels (LG for moderate and LhG for strong expression; Fig. S3C1, S3D).

Interestingly, our experiments indicate that stronger neuronal DNAJB6-expression extended lifespan in *D. melanogaster* expressing HttQ100-mRFP in neurons as compared to *D. melanogaster* expressing HttQ100-mRFP and a control (difference in T_{50} = 43%; Fig. 3B, S3F), while moderate neuronal DNAJB6-expression only affected a small sub-population of *D. melanogaster* (Fig. 3A, S3E), indicating that the protective DNAJB6-effects might be dependent on DNAJB6-protein levels.

This hypothesis is supported by previous data from our laboratory indicating that the sub-stoichiometric ratio of DNAJB6:polyQHtt determines the DNAJB6-ability to prevent polyQ-fibrillation *in vitro*.[4,11] The lifespan of control *D. melanogaster* lines was comparable to *D. melanogaster* expressing HttQ15-mRFP in neurons (Fig. 2B, S2C vs Fig.S3E, S3F), indicating that neither the combined use of multiple promoters, nor eGFP-expression affected *D. melanogaster* viability. Similarly, neuronal DNAJB6-expression did not affect the lifespan of *D. melanogaster* with neuronal expression of non-pathogenic HttQ15-mRFP (Fig. S3G). Together these data confirm that DNAJB6 has a specific, dose-dependent, cell-autonomous protective activity against polyQHtt-mediated neurotoxicity in *D. melanogaster*.

We have previously shown that DNAJB6 acts on the primary and secondary nucleation steps in the polyQ-initiated aggregation process and that it is associated with reduced polyQ-mediated neurodegeneration.[3,4] In line with these observations, we found that only stronger neuronal DNAJB6-expression (Fig.3C, Fig. S3H) reduced the HttQ100-mRFP-aggregate-load in total *D. melanogaster* head lysates.

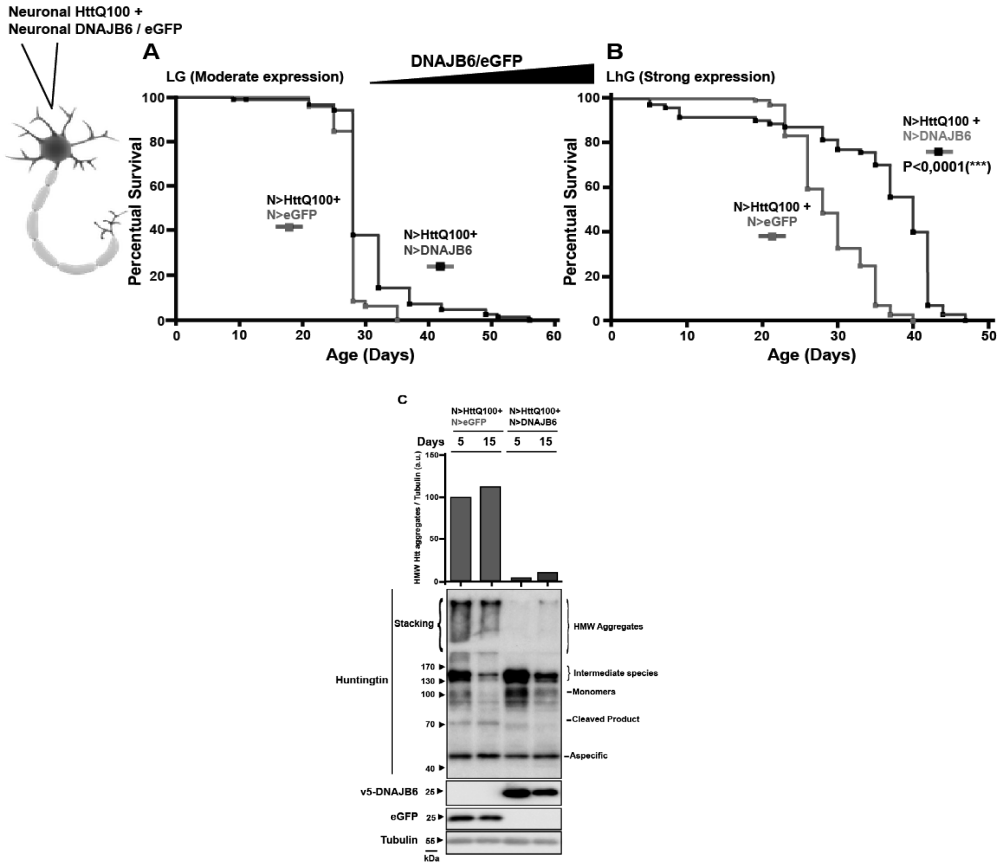

Figure 3: Lifespan and Htt-protein levels of D. melanogaster pan-neuronally expressing HttQ100-mRFP and DNAJB6. A, B) *Lifespan of isogenized D. melanogaster lines (♂) co-expressing neuronal (N) HttQ100-mRFP (Gal4-UAS) and neuronal (N) DNAJB6/eGFP (LexA-LexO) using the respective ELAV promoters. LexO-DNAJB6/eGFP expression was modulated (LG = moderate, 3A; LhG = stronger, 3B). Statistical significance was analyzed in ≈100 flies/group by the Log rank Mantel-Cox test. .Additional control lines, statistics and genotypes for Fig. 3A and Fig. 3B are shown in Fig. S3E and Fig. S3F, respectively.* ***C)*** *Representative Western blots of total head lysates of D. melanogaster (♀, 5 and 15 days old adults) co-expressing neuronal (N) HttQ100-mRFP (Gal4-UAS) and neuronal (N) DNAJB6/eGFP (LexA-LexO). Data for moderate LexO-DNAJB6/eGFP expression using ELAV-LG not shown. The anti-Htt antibody was used for HttQ100-mRFP-detection (100kDa = monomers, 70kDa = cleaved products, 130-170kDa = intermediate aggregate species, stacking gel = HMW aggregates). The anti-V5 antibody was used for V5-DNAJB6 detection and the anti-GFP antibody for eGFP detection. Tubulin as loading control. HMW aggregate quantification (signal in stacking gel normalized over tubulin) is shown for each line. Genotypes: 1) Control line (red): w(-); UAS HttQ100-mRFP*

/ ELAV LhG; ELAV Gal4 / LexO eGFP. 2) Rescued line (blue) w(-); UAS HttQ100-mRFP / ELAV LhG; ELAV Gal4 / LexO DNAJB6.

Astrocytes are glial cells that contribute to brain homeostasis and support neuronal functions through a pleiotropy of functions, including the provision of nutrients to neurons, the participation in neuronal signalling (tripartite synapse), and the release of brain factors.[12,13] Neuronal damage in HD, as well as in many other aggregate-related neurodegenerative diseases, leads to molecular, cellular, and functional astrocytic changes that are thought to be initially aimed at counteract the progression of neurodegeneration.[2] However, long-term stressors related to neurodegenerative diseases are known to result in severe and prolonged activation of astrocytes, eventually resulting in astrocytes assuming a 'reactive' phenotype, which is thought to be detrimental to the surrounding brain tissue and contribute to HD pathology.[14,15] Considering the delicate balance and importance of neuron-astrocyte interactions in the interpretation of our findings, we hypothesize that specific astrocytic HSP-overexpression may be capable of counteracting polyQHtt-aggregation and –toxicity and thereby protect neurons in a non-cell autonomous manner. To test this hypothesis, we selectively overexpressed human DNAJB6 in astrocyte-like cells via the ALRM-LexA promoter[16] or in all glial cells via the REPO-LexA promoter[17] in the background of *D. melanogaster* selectively expressing HttQ100-mRFP in neurons via ELAV-GAL4 (Fig. S3A-D).

To test the autonomy of our model system, we analyzed the brains of adult *D. melanogaster* co-expressing non-aggregating mCD8-RFP in neurons via the UAS-GAL4 system and eGFP in astrocyte-like cells via the LexA-system; confocal microscopy showed non-overlapping staining as evidenced by diffuse RFP fluorescence in neuronal lobes (e.g. antennal lobes, mushroom bodies) surrounded by a network of eGFP-positiveastrocytes with ramified processes (Fig. 4A). Brains of *D. melanogaster* expressing neuronal HttQ100-mRFP showed RFP-punctae reminiscent of aggregate formation that mainly localized to the antennal lobes and the area between the central brain complex and the optical lobes (Fig. 4B). Of note, unlike *D. melanogaster* expressing mCD8-RFP, a small fraction of eGFP-positive astrocytes in *D. melanogaster* expressing HttQ100-mRFP in neurons were observed to contain RFP-punctae as well (Fig 5B, 5C).

Strikingly, strong glial (via REPO-LhG) and astrocytic (ALRM-LhG) DNAJB6-expression significantly extended the lifespan of *D. melanogaster* expressing

HttQ100-mRFP in neurons, increasing the T50 by 23% and 25%, respectively (Fig. 4D, 4F, S4A). Mirroring our results in neurons, moderate expression of DNAJB6 via the LG promoters only provided an extension in lifespan in a small sub-set of *D. melanogaster* (Fig. 4C, 4E, S4B, S4C). Together these data indicate that DNAJB6-expression in glial cells –particularly in astrocytes- has specific, non-cell autonomous, dose-dependent, protective effects against polyQHtt-mediated toxicity.

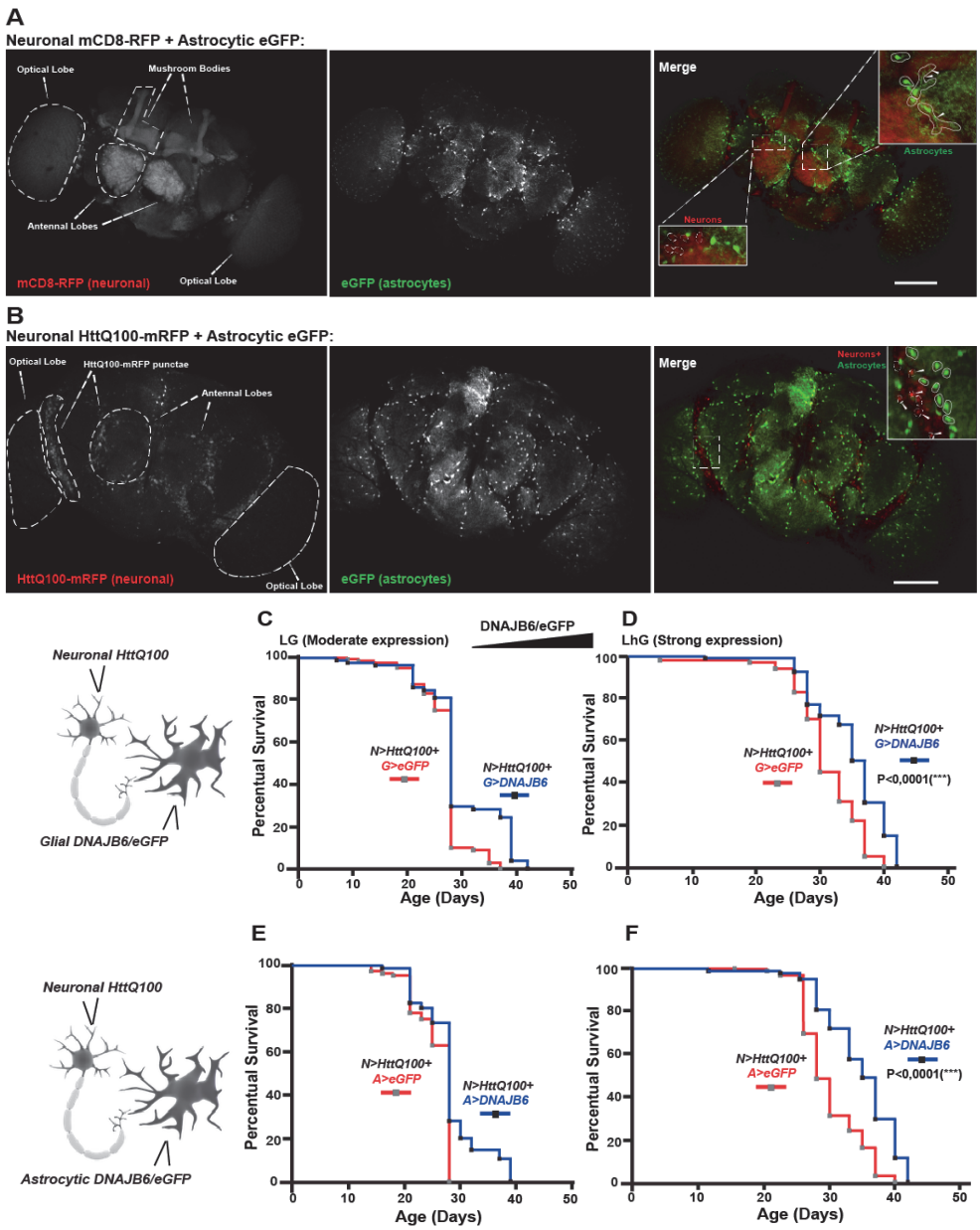

Figure 4: Immunofluorescence of D. melanogaster expressing eGFP in astrocyte like cells and mCD8-RFP or HttQ100-mRFP in neurons and the effects of glial and astrocytic DNAJB6-expression on lifespan in D. melanogaster expressing HttQ100-mRFP in neurons. A,B) *Representative confocal brain-images of D. melanogaster (♂, 15 days old adults) co-expressing transgenes in different cell types using the two independent expression systems: mCD8-RFP (4A) or HttQ100-mRFP (4B) in neurons (Gal4-UAS, ELAV) and eGFP in astrocytes (LhG-LexO, ALRM). Neuronal lobes and regions rich in HttQ100-mRFP punctae were enlarged. Neuronal cell bodies, astrocytic cell bodies (circles), and astrocytic processes (arrows, only in Fig. 4A) are indicated in the respective merges. Scale bar: 100 μm. Magnification: 20x. A minimum of 3 brains / condition were imaged and found to display similar expression patterns. Genotype: w(-); UAS mCD8-RFP(or UAS HttQ100-mRFP) / ALRM LhG; ELAV Gal4 / LexO eGFP.* ***C-F)*** *Lifespan of isogenized D. melanogaster lines (♂) co-expressing neuronal (N) HttQ100-mRFP (Gal4-UAS, ELAV) and glial (G) or astrocytic (A) DNAJB6/eGFP (LexA-LexO) using respectively REPO (4C, 4D) or ALRM (4E, 4F) promoters, respectively. LexO-DNAJB6/eGFP expression was regulated by the LG (moderate expression, Fig. 4C, 4E) or LhG (strong expression, 4D, 4F) promoters. Statistical significance was analyzed in ≈100 flies/group by Log rank Mantel-Cox test. Additional control lines, statistics, and genotypes are shown in Fig. S4A (LhG) and Fig. S4B (LG).*

To unravel the mechanism underlying the protective DNAJB6-mediated non-cell autonomous effects, we investigated whether glial or astrocytic DNAJB6-expression was associated with a reduction in the HMW HttQ100-mRFP-aggregate-load. However, unlike our results in *D. melanogaster* co-expressing DNAJB6 and polyQHtt in neurons (Fig.3B, Fig. 5A), astrocytic or glial DNAJB6-expression was not associated with a decreased HMW Htt-aggregate-load in total head lysates of *D. melanogaster* expressing HttQ100-mRFP in neurons. These findings suggest that intercellular transport of DNAJB6 from glia cells to neurons is unlikely to underlie the DNAJB6-mediated non-cell autonomous protective effects as suggested by the literature (Fig.S5A).[18]

Literature indicates that polyQHtt aggregates may propagate from neuron to neuron in a prion-like manner, thereby contributing to the progression of neurodegeneration.[19–22] Glial cells might restrict such spreading by taking up these prion-like protein species from the extra-cellular space before it can enter and infect adjacent neurons.[19] The progressive uptake and accumulation of toxic Htt-species by glial cells is known to increase astrocytic stress, eventually resulting in a general loss of glial functions, reactive astrocytosis, and neuroinflammation.[14,15,23] Interestingly, the astrocytic expression of HttQ100-

mRFP in *D. melanogaster* via the specific ALRM-Gal4 promoter was associated with a reduction in *D. melanogaster* lifespan, implying that astrocytic polyQ-Htt may contribute to the neurodegenerative phenotype (Fig. S5C).

An alternative explanation for the positive effects of astrocytic or glial DNAJB6-expression on the lifespan of *D. melanogaster* pan-neuronally expressing HttQ100-mRFP may be DNAJB6-mediated protection of astrocytes/glia against polyQHtt-aggregate- toxicity, thereby enabling these cells to either promote neuronal fitness or to actively prevent the propagation of aggregates from one neuron to the next by enhancing astrocytic polyQHtt-uptake capabilities (Fig. S5B3). Although our model system was not designed to investigate the effects of DNJAB6 on neuron-to-neuron polyQHtt-propagation, our confocal microscopy analysis revealed that ~10% of all astrocytes expressing eGFP in *D. melanogaster* co-expressing HttQ100-mRFP in neurons contained mRFP-positive punctae (Fig. 5B3-4, 5C, S5D). The presence of these mRFP-positive punctae was not due to indiscriminate protein transfer, as proven by the absence of mRFP-positive punctae in eGFP-positive astrocytes of *D. melanogaster* expressing neuronal non-aggregating membrane-bound mCD8-RFP (Fig. 5B1-2, 5C, S5D). Taken together, these results suggest that the presence of HttQ100-mRFP-punctae in astrocytes is the result of active, inter-cellular, aggregate-progression. Importantly, the combined expression of neuronal HttQ100-mRFP and astrocytic DNAJB6 resulted in a significant increase of astrocytes displaying mRFP-positive punctae to ~50% (Fig. 5B5-6, 5C, S5D).

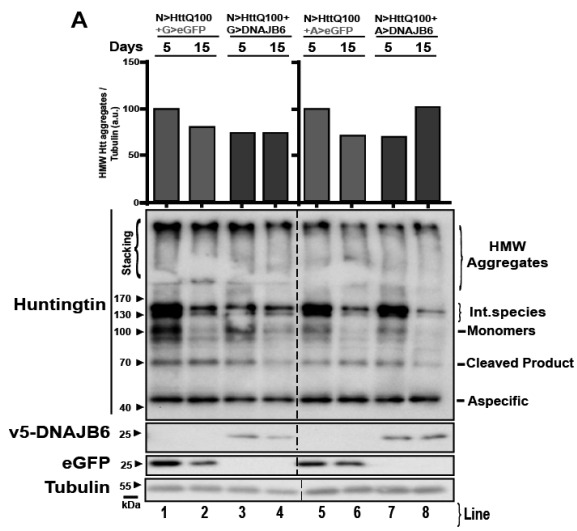

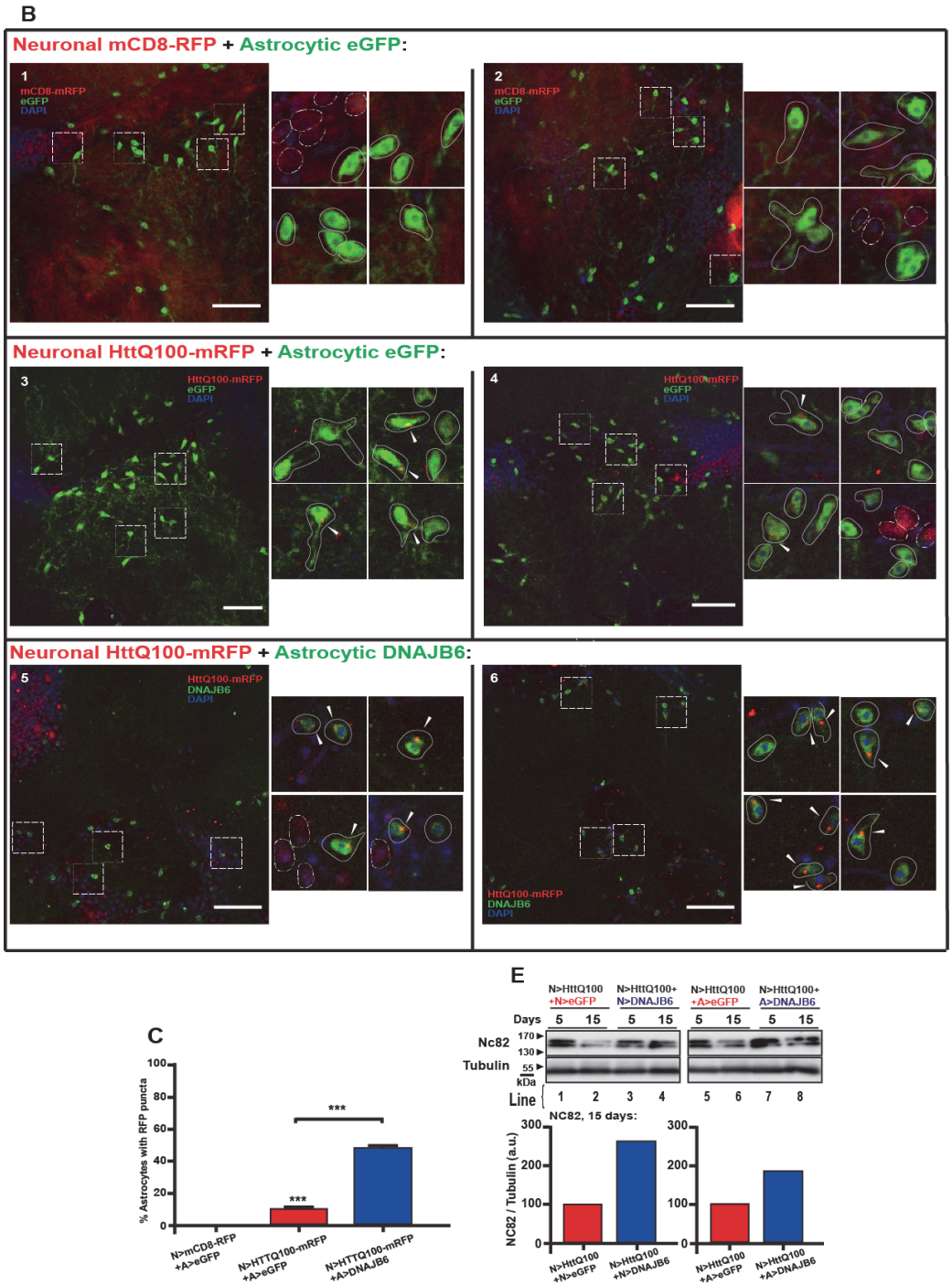

Figure 5: Effect of glial/astrocytic DNAJB6-expression on polyQHtt aggregate formation, aggregate transmission, and overall neuronal viability in D. melanogaster expressing HttQ100-mRFP in neurons. A) *Representative Western*

blots of total head lysates from D. melanogaster lines (♀, 5 and 15 days old adults) co-expressing neuronal HttQ100-mRFP (N, Gal4-UAS) and glial (G, line 1-4) or astrocytic (A, line 5-8) DNAJB6/eGFP (LexA-LexO) via REPO or ALRM promoters (LhG version), respectively. The anti-huntingtin antibody was used HttQ100-mRFP detection (100kDa = monomers, 70kDa = cleaved products, 130-170kDa = intermediate aggregate species, stacking gel = HMW aggregates) and the anti-V5 antibody for V5-DNAJB6 detection. The anti-GFP antibody was used for eGFP detection and Tubulin was used as loading control. HttQ100-mRFP-HMW aggregates were normalized over tubulin and quantified for each line. Genotypes: 1) Control line (red): w(-); UAS HttQ100-mRFP / Driver LhG; ELAV Gal4 / LexO eGFP. 2) Rescued line (blue): w(-); UAS HttQ100-mRFP / Driver LhG; ELAV Gal4 / LexO DNAJB6. ***B)*** *Representative confocal images of D. melanogaster brains (♂, 15 days old adults) in lines co-expressing neuronal transgenes (mCD8-RFP / HttQ100-mRFP, Gal4-UAS) via ELAV and astrocytic transgenes (DNAJB6b/eGFP, LhG-LexO) via ALRM. Two representative images from the central brain region indicated in Fig. S5D were taken for each indicated condition and magnified details shown. In magnified details, neurons (dashed circles), astrocytes (continued line circles), HttQ100-mRFP punctae in astrocytes (arrow), used for counting in 5C, are shown. The anti-V5 antibody was used for V5-DNAJB6 detection, Alexa488 was used as secondary antibody. Scale bar: 25 μm. Magnification: 63x. A minimum of 3 brains / condition with 20 sections (≈3 μm) in the central brain area indicated in S5D were imaged with similar patterns of expression levels being observed. Genotypes: 1) Control (Fig. 5B1 and 5B2): w(-); UAS CD8-mRFP / ALRM LhG; ELAV Gal4 / LexO eGFP. 2) Condition 1 (Fig. 5B3 and 5B4): w(-); UAS HttQ100-mRFP / ALRM LhG; ELAV Gal4 / LexO eGFP. 3) Condition 2 (Fig. 5B5 and 5B6): w(-); UAS HttQ100-mRFP / ALRM LhG; ELAV Gal4 / LexO DNAJB6.* ***C)*** *Percentage of green fluorescent astrocytes containing mRFP-positive punctae in a confocal section in D. melanogaster brains from Fig. 5B. All green fluorescent astrocytes containing or not containing mRFP-positive punctae in each of 20 confocal sections (≈3 μm) of the central brain area in Fig. S5D, 2 brains/condition were considered for counting. Statistical significance analyzed by 1-way ANOVA test (SEM, ***, p<0,001).* ***E)*** *Representative Western blots of total head lysates of D. melanogaster lines (♀, 5 and 15 days old adults) co-expressing neuronal HttQ100-mRFP (N, Gal4-UAS) and neuronal (N) or astrocytic (A) DNAJB6/eGFP (LexA-LexO) via ELAV (line 1-4) or ALRM (line 5-8) LhG-promoters, respectively. The anti-NC82 antibody was used for NC82-detection and Tubulin as loading control. Quantification of NC82 normalized over tubulin shown for each line at day 15 . Genotypes: 1) Control line (red): w(-); UAS HttQ100-mRFP / Driver LhG; ELAV Gal4 / LexO eGFP. 2) Rescued line in blue w(-); UAS HttQ100-mRFP / Driver LhG; ELAV Gal4 / LexO DNAJB6.*

Our results thus support findings that astrocytes are capable of taking up polyQHtt-aggregate species that are selectively expressed in neurons[23] and furthermore provide compelling evidence that astrocytic expression of DNAJB6 may increase the astrocytic ability to take up polyQHtt-aggregates and/or the astrocytic resistance against polyQHtt-mediated toxicity, thereby potentially slowing down the progression of polyQHtt-neurotoxicity.

To assess overall neuronal fitness, we analyzed total *D. melanogaster* head lysates for neuronal NC82 (marker: pre-synaptic active zone).[24] We found that NC82 levels were strongly reduced in 15 day-old *D. melanogaster* neuronally expressing HttQ100-mRFP(Fig.S5E). Interestingly, neuronal –as well as astrocytic-DNAJB6-expression in *D. melangoaster* expressing HttQ100-mRFP in neurons was associated with higher levels of NC82, further supporting the notion that DNAJB6 improves overall neuronal fitness cell autonomously and non-cell autonomously.

Our experiments verified that the expression of a HSPs in glia -and astrocytes in particular- protects neurons beyond maintaining astrocytic functions to support neuronal health and control neuro-inflammation[2,14,15] Our results indicate that astrocytic DNAJB6-overexpression protects *D. melanogaster* against polyQHtt-aggregation and –toxicity non-cell autonomously, resulting in the lifespan extension of *D. melanogaster* pan-neuronally expressing mRFP-HttQ100. Our data further support the idea that polyQHtt-aggregates may progress from neurons to astrocytes.[19–22] These data suggest that astrocytes may serve as reservoir for toxic, prion-like, aggregate-inducing, species, thereby potentially preventing their progressive neuronal spread and neurodegeneration.

However, the reservoir capacity of astrocytes is limited as internalized aggregates convey their toxicity to astrocytes by recruiting non-toxic polyQHtt-conformers and PQC components. By preventing the primary and secondary nucleation steps in the Htt-aggregation process,[4,11] DNAJB6 may enhance astrocytic resistance to aggregate toxicity, thereby increasing astrocytic reservoir capacity. Our data further show that the DNAJB6-mediated effects contribute to overall neuronal fitness *in vivo*. Considering the reciprocal neuron-astrocyte interactions, a combination of DNAJB6-mediated effects may support neuronal viability, including enhanced astrocytic resistance to polyQHtt-toxicity and the promotion of neuronal fitness. Based on our data, we further hypothesize that the increased prion-reservoir capacity of DNAJB6-expressing astrocytes may impede on the progressive neuronal polyQHtt-aggregate propagation in the brain.

Materials and Methods

Vectors

UAS/LexO vectors were obtained by cloning the sequences of HttQ15-mRFP or HttQ100-mRFP (mutant Htt exons 1-12, biologically relevant cleaved product of the mutant protein with a pathogenic poly(Q) tract and multiple sites of protein interactions[8])_or V5-DNAJB6 (short nuclear and cytosolic isoform B[6])) or eGFP (a reporter of internal retinal integrity[7], Clontech) into the multiple cloning site of pUAS *attB* or pLexO *attB* (kindly provided by Prof. K. Basler Group, UZH). Driver (Promoter cell-specific expression) vectors were generated based on the backbone of the pDPP-Gal4 *attB* or pDPP-LG *attB* or pDPP-LhG *attB* plasmids (Prof. K. Basler Group, UZH). The DPP promoter was substituted with the sequence of the ELAV (pan-neuronal, from pELAV-Casper vector, kindly provided by Prof. Liqun Luo, Stanford University), REPO (pan-glial, from pENTRY-D-TOPO-REPO4.3 vector, kindly provided by Prof. C. Klämbt, University of Münster), or ALRM (astrocytic, from pALRM-Casper vector, kindly provided by Prof. M. Freeman, UMASS) promoters. All vector sequences were confirmed via sequencing. Please refer to the table in Table S1 for a complete vectors list.

D. melanogaster stocks

The *D. melanogaster* lines listed in Table S1 were obtained via embryo injection and transformation with the above mentioned *attB* vectors by Best Gene Inc. injection service, facilitating the *attP*-site specific PhiC31 integrase system. In addition, the following *D. melanogaster* lines from the Bloomington Drosophila Stock Center were used: *w(-); +/+; GMR-Gal4* (Line #8121); *w(-); +/+; UAS-mCD8-GFP* (Line #5130); *w(-); UAS-mCD8-RFP*; +/+ (Line #27391). All lines used for this study were isogenized via backcrossing with the control stock w^{1118}-line for 6 generations to remove any background mutations.

Line Name	Plasmid	*D.melanogaster* Genotype	Chromosome	Chromosome Arm	PhiC31 *attP* -Site
Driver (Cell-Specific) Lines					
ELAV-Gal4	p ELAV-Gal4 *attB*	*w(-); +/+; ELAV-Gal4*	3	R	ZH-attP-86Fb
ALRM-Gal4	p ALRM-Gal4 *attB*	*w(-); +/+; ALRM-Gal4*	3	R	ZH-attP-96E
ELAV-LG	p ELAV-LG *attB*	*w(-); ELAV-LG; +/+*	2	L	ZH-attP-22A
ELAV-LhG	p ELAV-LhG *attB*	*w(-); ELAV-LHG; +/+*	2	L	ZH-attP-22A
REPO-LG	p REPO-LG *attB*	*w(-); REPO-LG; +/+*	2	L	ZH-attP-35B
REPO-LhG	p REPO-LhG *attB*	*w(-); REPO-LHG; +/+*	2	L	ZH-attP-35B
ALRM-LG	p ALRM-LG *attB*	*w(-); ALRM-LG; +/+*	2	L	ZH-attP-35B
ALRM-LhG	p ALRM-LhG *attB*	*w(-); ALRM-LHG; +/+*	2	L	ZH-attP-35B
UAS/LexO-TRANSGENE Lines					
Uas HttQ15-mRFP	p Uas HttQ15-mRFP *attB*	*w(-); Uas HttQ15-mRFP; +/+*	2	R	ZH-attP-51C
Uas HttQ100-mRFP	p Uas HttQ100-mRFP *attB*	*w(-); Uas HttQ100-mRFP; +/+*	2	R	ZH-attP-51C
Uas DNAJB6b	p Uas V5-DNAJB6b *attB*	*w(-); Uas V5-DNAJB6b; +/+*	2	R	ZH-attP-58A3
Uas eGFP **(D)**	p Uas eGFP *attB*	*w(-); Uas eGFP; +/+*	2	R	ZH-attP-58A3
LexO V5-DNAJB6b	p LexO V5-DNAJB6b *attB*	w(-);+/+; LexO V5-DNAJB6b	3	L	ZH-attP-68E1
LexO eGFP **(A)**	p LexO eGFP *attB*	w(-);+/+; LexO eGFP	3	L	ZH-attP-68E1
LexO eGFP **(B)**	p LexO eGFP *attB*	w(-);+/+; LexO eGFP	3	L	ZH-attP-62B
LexO eGFP **(C)**	p LexO eGFP *attB*	w(-);+/+; LexO eGFP	3	L	ZH-attP-75D

Table S1*. D.melanogaster lines generated by embryo-injection and -transformation with attB plasmids by Best Gene Inc, using the attP-site specific PhiC31 integrase system.*

D. melanogaster stock maintenance

All stocks and experimental flies were kept in polystyrene vials 25x95 mm filled with 8 ml/vial of solidified media (17 g/l Agar; 26 g/l Yeast; 54 g/l Sugar; 1.3 mg/l Nipagin). All experimental flies were maintained in a humidified and temperature controlled incubators at 25 °C on a 12 hours light/dark cycle (Premium ICH Insect Chamber, Snijders Labs). Experimental flies were anesthetized on a CO^2 pad and selected according to their gender and phenotype by light microscopy.

Lifespan curves, climbing assay and fitness score

Parental flies (5-6 females and 5-6 males) were kept in vials for 3 days and then removed. All virgin offspring flies were collected within the same 24 hours. For each analyzed group, ≈100 flies were collected according to specific gender and phenotype and collected and kept in new vials (10 flies/vial). Flies were transferred to new vials containing fresh medium every 2 days; deaths were scored daily. Statistical significance of lifespan curve-differences were analyzed by Log rank (Mantel-Cox) test and Gehan-Breslow-Wilcoxon test using the Graph Pad Prism Software Version 5.00. All curve-comparisons were calculated on flies analyzed within the same experiment. The T50 was defined as the time point at which 50% of the initial *D. melanogaster* population had died. Climbing assays were performed on the same flies used in the survival analysis. To assess *D. melanogaster* climbing ability, fly vials were inserted into a rack and forced to the bottom via tapping. Photos were taken (at tap, after 5 seconds, after 20 seconds, repeated three times for each vial) and used to calculate % climbers for each condition at each time point. Climber flies were defined as flies able to climb further than 1.2 cm from the bottom after the tap (limit established in a control experiment). Fitness scores were calculated for each time point using the following formula: % climbers x survival proportion (from lifespan curves) / 100. Statistical significance of fitness score-differences was assessed at each time point and analyzed by 2-way ANOVA using Graph Pad Prism Software Version 5.00.

Antibodies and reagents

Antibodies (dilutions indicated in brackets for Western blots (WB) and Immunofluorescence (IF)) against huntingtin (Chemicon, MAB2166, WB 1:5000), eGFP (Clontech-Living Colors, cat. No.632375, WB 1:5000), α-tubulin (Sigma Aldrich, clone DM1A, WB 1:2000), V5 epitope tag in DNAJB6b (Thermo Fisher Scientific, cat. No.R960-25, IF 1:50), Draper (DSHB, clone 8A1, IF 1:50), NC-82 (DSHB, WB 1:5000, IF 1:50) were used. The following chemicals were used: DAPI for nucleic staining (Thermo Fisher Scientific, cat. No. D1306). 20% SDS Solution (BioRad, cat. No.n1610418). PBS

components (NaCl cat. No.S9888, KCl cat. No. P9541, Na^2HPO^4 cat. No. 255793, KH^2PO^4 cat. No. V000225), Tween-20 (cat. No. P2287), Triton X-100 (cat. No. T8787), Bovine Serum Albumin (cat. No. A2058, BSA), glycerol (cat. No. G5516), 3.7% Formaldehyde (cat. No. 11-0705 SAJ), Tris base (cat. No. T1503), and β-mercaptoethanol (cat. No. M6250) were from Sigma Aldrich.

Western blotting of *D. melanogaster* total head lysates

30-40 *D. melanogaster* adults with the same phenotype, gender, and age (days after pupal eclosion) were collected per experimental condition; following freezing in liquid nitrogen and vortexing, separated heads were collected, counted and lysed in SDS-rich buffer (SDS 1.45%, Glycerol 20%; Tris Base 0.2 M. 2.5 μl of buffer/head) via sonication (3 pulses of 50 Watt for 5 seconds). The homogenized lysate was centrifuged at 1000 xg for 3 seconds to separate the cuticle debris from the surnatant. The protein-containing surnatant was collected, quantified via spectrophotometry (Implen NanoPhotometer UV/Vis), and equalized. Samples were supplied with 5% β-mercaptoethanol and bromophenol blue and boiled at 99 °C for 5 minutes. Equal amounts of sample volumes were resolved on SDS-PAGE. Flies stemming from the same line were collected from different vials; the entire experiment was repeated at least twice.

Western blotting and protein quantification

Following sample-preparation, proteins were resolved by SDS-PAGE, transferred to nitrocellulose membranes, and processed for Western blotting. Primary antibodies (concentrations mentioned above) were prepared in 3% BSA/0.1%, PBS-Tween 20 and secondary antibodies (1:5000, Invitrogen, horse peroxidase conjugated to IGG or IGM) in 5% milk/0.1% PBS-Tween 20. Membranes were incubated with Pierce ECL Western blotting substrate (cat. No. 32106) for 2 minutes and visualized using ChemiDoc Touch Imaging System (BioRad). Blots were quantified via the Image Lab Version 5.2.1 software (BioRad).

Imaging of fluorescent eyes in *D.melanogaster* and quantification

Experimental *D. melanogaster* adults with the same phenotype, gender, and age (days after pupal eclosion) were collected for each and anesthetized on a CO^2 pad while their GFP-fluorescent eyes were visualized using a Leica MZ10 F Fluorescence stereomicroscope (GFP3 filter). 10 eyes from different flies were visualized per condition; GFP fluorescence was quantified using the Image J 1.48v software and expressed as corrected by mean eye fluorescence (CMEF). CMEF was calculated as integrated density (selected area x mean background fluorescence). Statistical significance of CMEF differences were analyzed by 1-way ANOVA using Graph Pad Prism Software Version 5.00.

D.melanogaster Immunofluorescence (IF), Imaging and Punctae Quantification

Brains of experimental *D. melanogaster* adults were collected according to phenotype, gender, age (days after pupal eclosion), and condition, incubated in 0.1% Triton X-100 / 1x PBS buffer, fixed in 3.7% Formaldehyde / 0.1% Triton X-100 / 1 x PBS buffer for 20 minutes at room temperature. Following the blocking of non-specific sites using 2% BSA / 0.1% Triton X-100 / 1x PBS buffer for 30 minutes at room temperature, samples were incubated with the primary antibody (dilution 1:50) in blocking buffer for 2 days at 4°C and visualized by incubation with species-specific secondary Alexa-conjugated antibody dyes (Invitrogen, Alexa Fluor 488 goat-anti-mouse; dilution 1:500) and DAPI (final concentration 0.2 μg/μl) in blocking buffer for 2 days at 4°C, to visualize primary antibodies and nuclei, respectively. Brains were embedded in mounting solution (CitiFluor®, Agar Scientific) and mounted between glass slide and coverslip; visualization occurred via confocal microscopy within 24 hours. IF images of *D. melanogaster* brains were captured using a confocal laser scanning microscope (Leica TCS SP8) with a 63x/1.40 objective lens. Z-stack images were obtained to investigate punctae at different Z-planes in cells. Cellular punctae-quantification was carried out manually. Photoshop and Image J were used for image processing. Statistical significance of value-differences were analyzed by 1-way ANOVA using Graph Pad Prism Software Version 5.00.

Supplementary information

FIGURE S1

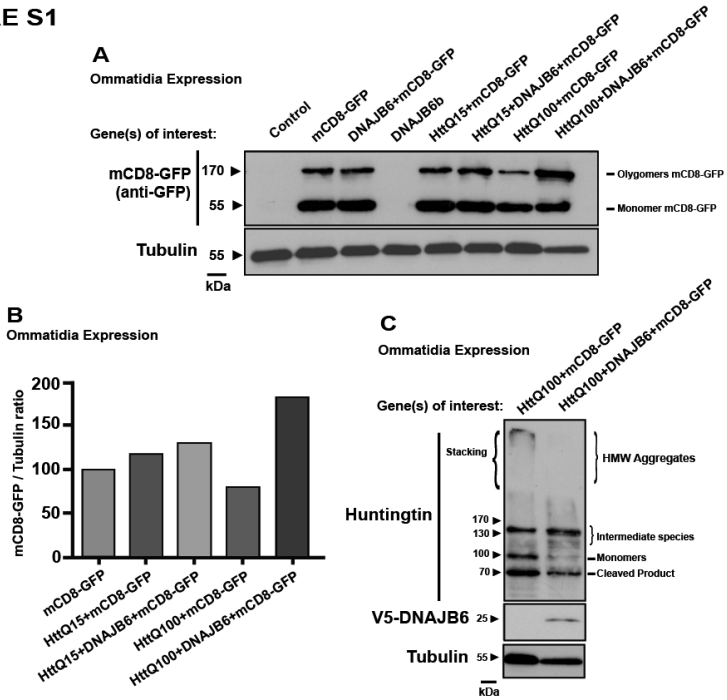

Figure S1. A) *Representative Western blots of total D. melanogaster head lysates (♀, Gal4-UAS system, 48 hours old adults) with GMR-driven expression of the indicated transgenes in ommatidia. The anti-GFP antibody was used to detect mCD8-GFP (bands at ~170 and ~55 kDa for oligomers and monomers of mCD8-GFP respectively) and tubulin was used as loading control. Genotypes: w(-); UAS Htt (Q15-mRFP or Q100-mRFP) / + (or UAS V5-DNAJB6); GMR Gal4 / UAS mCD8-GFP.* ***B)*** *Quantification of mCD8-GFP protein levels (total signal from bands at ~170 and ~55 kDa for oligomers and monomers of mCD8-GFP respectively) normalized for tubulin.* ***C)*** *Representative Western Blots of total head lysates (♀, Gal4-UAS system, 48 hours old adults) expressing the indicated transgenes in ommatidia via GMR. The anti-Htt antibody was used to detect HttQ100-mRFP-monomers (100 kDa), cleaved HttQ100-mRFP-products (70 kDa), intermediate HttQ100-mRFP-aggregate species (130-170 kDa), and HMW HttQ100-mRFP-aggregates (stacking gel). The anti-V5 antibody was used to detect V5-DNAJB6. Tubulin was used as loading control. Genotypes: w(-); UAS HttQ100-mRFP / + (or UAS V5-DNAJB6); GMR Gal4 / UAS mCD8-GFP.*

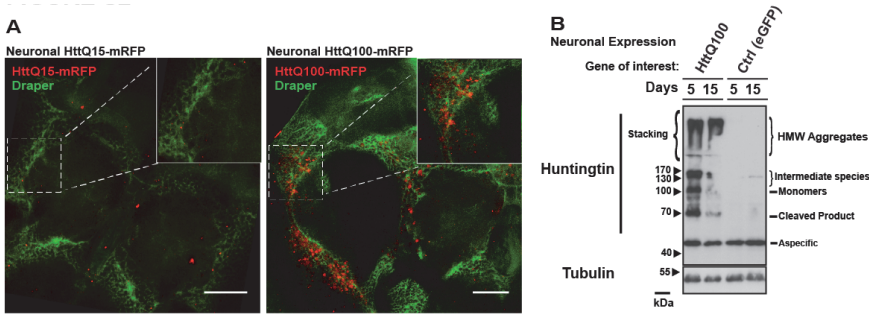

C
Neuronal Expression

LINE	GENOTYPE	#DEATHS	MEDIAN SURVIVAL	COMPARISON	TEST 1	TEST 2
ELAV Gal4> +	w(-); +/+; ELAV Gal4/+	91	72			
ELAV Gal4> uas eGFP	w(-); uas eGFP/+; ELAV Gal4/+	92	71	eGFP vs +	ns	ns
ELAV Gal4> uas HTTQ15	w(-); uas HttQ15/+; ELAV Gal4/+	86	64	HttQ15 vs eGFP	*	*
ELAV Gal4> uas HTTQ100	w(-); uas HttQ100/+; ELAV Gal4/+	95	29	HttQ100 vs HttQ15	Significant, P<0,0001 (***)	Significant, P<0,0001 (***)

TEST 1: LOG RANK (Mantel-Cox) Test
TEST 2: Gehan-Breslow-Wilcoxon Test

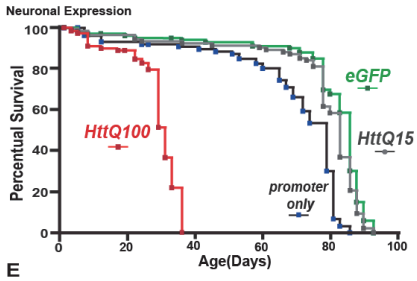

E
Neuronal Expression

LINE	GENOTYPE	#DEATHS	MEDIAN SURVIVAL	COMPARISON	TEST 1	TEST 2
ELAV Gal4> +	w(-); +/+; ELAV Gal4/+	87	79			
ELAV Gal4> uas eGFP	w(-); uas eGFP/+; ELAV Gal4/+	99	86	eGFP vs +	Significant, P<0,0001 (***)	Significant, P<0,0001 (***)
ELAV Gal4> uas HTTQ15	w(-); uas HttQ15/+; ELAV Gal4/+	98	83	HttQ15 vs eGFP	*	*
ELAV Gal4> uas HTTQ100	w(-); uas HttQ100/+; ELAV Gal4/+	96	31	HttQ100 vs HttQ15	Significant, P<0,0001 (***)	Significant, P<0,0001 (***)

TEST 1: LOG RANK (Mantel-Cox) Test
TEST 2: Gehan-Breslow-Wilcoxon Test

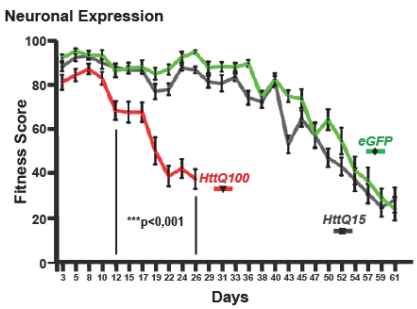

Figure S2. A) *Representative confocal images of D. melanogaster heads (♂, Gal4-UAS system, 15 days old adults, antennal lobe region) in lines with pan-neuronal expression of HttQ15-mRFP or HttQ100-RFP (using ELAV) stained for Draper (marker for glial cells, Alexa488, green). Scale bar: 50 µm. Magnification: 40x. Similar expression patterns were observed in a minimum of 3 brains/condition. Genotypes: w(-); UAS Htt (Q15-mRFP or Q100-mRFP) /+; ELAV Gal4/+.* ***B)*** *Representative Western blots of total D. melanogaster head lysates (♀, Gal4-UAS system, 5 and 15 days old adults)*

expressing the indicated transgenes using ELAV. The anti-Htt antibody was used to detect HttQ100-mRFP species (100kDa-mononomers, 70kDa-cleaved products, 130-170kDa-intermediate aggregate species, HMW aggregates in stacking gel), Tubulin was used as loading control. Genotypes: w(-); UAS HttQ100-mRFP (or UAS eGFP) / +; ELAV Gal4/+. ***C)*** *Genotype and statistical analysis of lifespan curves.* ***D)*** *Lifespan of isogenized D. melanogaster lines (♀, Gal4-UAS system) expressing HttQ100-mRFP or control transgene (HttQ15-mRFP, eGFP or only promoter)using ELAV. Statistical significance was analyzed in ≈100 flies/group by Log rank Mantel-Cox test. Please, refer to S2E for detailed statistics and genotypes.* ***E)*** *Genotype and statistical analysis of lifespan curves Fig. S2D.* ***F)*** *Fitness score of D. melanogaster lines Fig. 2B. Statistical significance was analysed in ≈100 flies/group by 2-way ANOVA, *** p<0,001.*

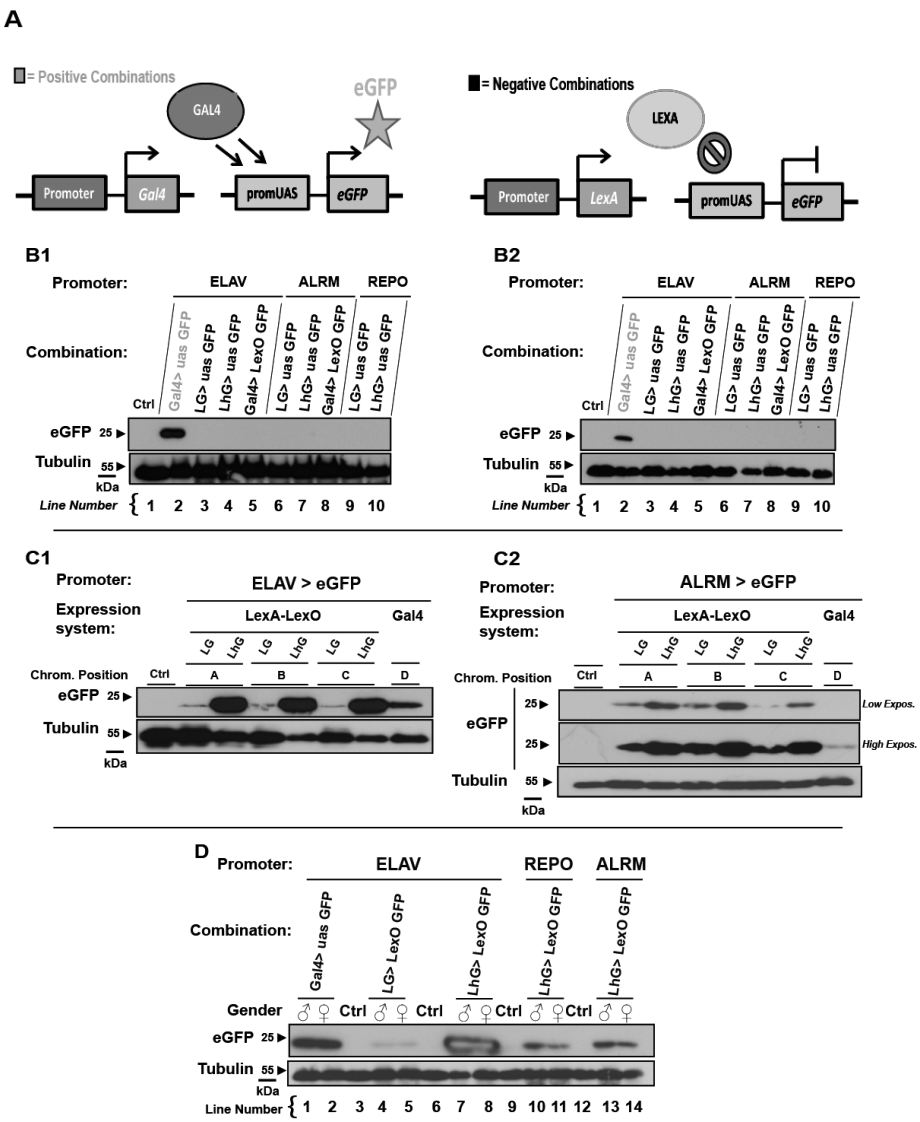

E

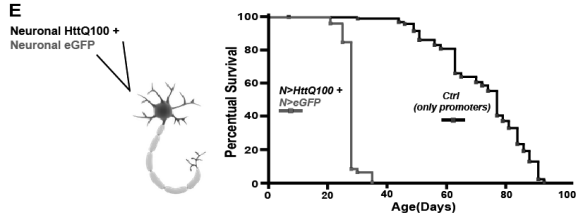

NR	LINE	GENOTYPE	#DEATHS	MEDIAN SURVIVAL	COMPARISON	TEST 1	TEST 2
1	*ELAV Gal4> +; ELAV LG>+*	*w(-); ELAV LG/+; ELAV Gal4/+*	94	77			
2	*ELAV Gal4> uas HTTQ100; ELAV LG>LexO eGFP*	*w(-); uas Httt Q100/ELAV LG; ELAV Gal4/LexO eGFP*	98	28	nr 2 vs nr 1	Significant,P<0,0001(***)	Significant,P<0,0001(***)
3	*ELAV Gal4> uas HTTQ100; ELAV LG>LexO DNAJB6b*	*w(-); uas Httt Q100/ELAV LG; ELAV Gal4/LexO DNAjb6b*	85	28	nr 3 vs nr 2	Significant,P<0,0001(***)	Significant,P<0,0001(***)

TEST 1: LOG RANK (Mantel-Cox) Test
TEST 2: Gehan-Breslow-Wilcoxon Test

F

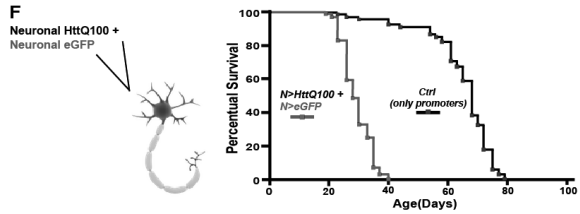

NR	LINE	GENOTYPE	#DEATHS	MEDIAN SURVIVAL	COMPARISON	TEST 1	TEST 2
1	*ELAV Gal4> +; ELAV LhG>+*	*w(-); ELAV LhG/+; ELAV Gal4/+*	68	68			
2	*ELAV Gal4> uas HTTQ100; ELAV LhG>LexO eGFP*	*w(-); uas Httt Q100/ELAV LhG; ELAV Gal4/LexO eGFP*	101	28	nr 2 vs nr 1	Significant,P<0,0001(***)	Significant,P<0,0001(***)
3	*ELAV Gal4> uas HTTQ100; ELAV LhG>LexO DNAJB6b*	*w(-); uas Httt Q100/ELAV LhG; ELAV Gal4/LexO DNAjb6b*	70	40	**nr 3 vs nr2**	Significant,P<0,0001(***)	Significant,P<0,0001(***)

TEST 1: LOG RANK (Mantel-Cox) Test
TEST 2: Gehan-Breslow-Wilcoxon Test

G

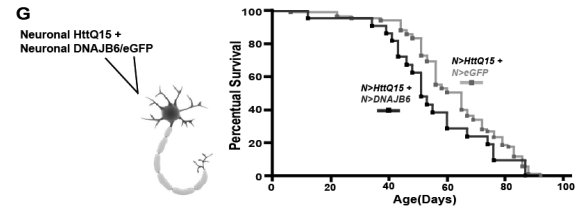

NR	LINE	GENOTYPE	#DEATHS	MEDIAN SURVIVAL	COMPARISON	TEST 1	TEST 2
1	*ELAV Gal4> uas HTTQ15; ELAV LHg>LexO eGFP*	*w(-); uas Httt Q15/ELAV LHg; ELAV Gal4/LexO eGFP*	85	65			
2	*ELAV Gal4> uas HTTQ15; ELAV LHg>LexO DNAJB6b*	*w(-); uas Httt Q15/ELAV LHg; ELAV Gal4/LexO DNAjb6b*	21	51	**2 vs 1**	ns	Significant (*, p=0,0302)

TEST 1: LOG RANK (Mantel-Cox) Test
TEST 2: Gehan-Breslow-Wilcoxon Test

H

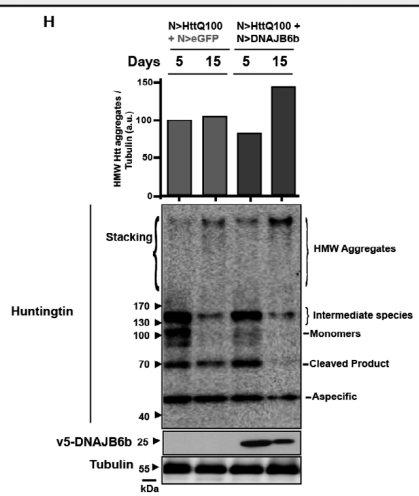

Figure S3 A-D. A) *Schematic overview of the Gal4-UAS and LexA-LexO expression systems in D. melanogaster: GFP-protein levels verify that GAL4 recognizes the UAS sequence, whereas the absence of GFP-protein levels confirms that LexA (LG or LhG) cannot recognize the UAS sequence and Gal4 cannot recognize the LexO sequence.* ***B-D)*** *Experimental confirmation of the autonomy of the Gal4-UAS and LexA-LexO expression systems.* ***B)*** *Representative Western blots of total head lysates of D. melanogaster lines (♂ in B1 and ♀ in B2, 15 days old adults) with transgene UAS-eGFP or LexO-eGFP-expression driven either by the Gal4 or LexA (LG or LhG) promoter. The presence (green) and absence (black) of GFP-expression are shown. The anti-GFP antibody was used for eGFP detection and Tubulin was used as loading control. ELAV: Lines 2-5. REPO: Lines 9-10; ALRM: Lines 6-8. Genotypes: w(-); UAS eGFP (D) /+; Driver Gal4/+ (positive combinations). w(-); UAS eGFP/ Driver LexA; +/+ or w(-); Driver Gal4/+; LexO eGFP (A) /+ (negative combinations).* w^{1118} *(negative control).* ***C)*** *Representative Western blots of total head lysates of D. melanogaster lines (♂, 15 days old adults) with UAS-eGFP or LexO-eGFP transgene-expression being driven by the Gal4 or LexA promoters, respectively. eGFP protein expression levels driven by the moderate LG promoter or stronger LhG promoter are shown. The anti-GFP antibody was used for eGFP detection and Tubulin was used as loading control. ELAV: C1. ALRM: C2. eGFP lines with different chromosome insertion positions are shown (see also Table S1). Genotypes: w(-); UAS eGFP/+; Driver Gal4/+ or w(-); Driver LexA (LG or LhG)/+; LexO eGFP/+. Negative ctrl line:* w^{1118}. ***D)*** *Representative Western blots of total head lysates of D. melanogaster lines (♂ and ♀, 15 days old adults with UAS-eGFP or LexO-eGFP transgene-expression being driven by the Gal4 or LexA promoters, respectively. Levels of eGFP expression among genders and different promoters are shown. The anti-GFP antibody for eGFP detection and Tubulin was used as loading control. ELAV: lines 1-8. REPO: lines 10-11; ALRM: lines 13-14. Genotypes: w(-); UAS eGFP(D)/+; Driver Gal4/+ or w(-); Driver LexA (LG or LhG)/+; LexO eGFP(A)/+. Negative ctrl line:* w^{1118}.

Figure S3 E-G. E) *Lifespan of isogenized D. melanogaster additional control lines (♂), statistics and genotypes for experiment in Fig. 3A (LexO-DNAJB6/eGFP with LG-moderate expression).* ***F)*** *Lifespan of D. melanogaster additional control lines (♂, 25°C), statistics and genotypes for experiment in Fig. 3B (LexO-DNAJB6/eGFP with LhG-strong expression).* ***G)*** *Lifespan, statistics and genotypes of D. melanogaster lines (♂), co-expressing neuronal (N) HttQ15-mRFP (Gal4-UAS) and neuronal (N) DNAJB6/eGFP (LexA-LexO) in neurons (using the respective ELAV promoters). Strong expression of LexO-DNAJB6/eGFP using ELAV-LhG promoter. Statistical significance analyzed with Log rank Mantel-Cox test.* ***H)*** *Representative Western blot of total head lysates of D. melanogaster lines (♀, 5 and 15 days old adults) co-expressing neuronal (N) HttQ100-mRFP (Gal4-UAS) and neuronal (N) DNAJB6/eGFP (LexA-LexO). Data shown are for moderate expression of LexO-DNAJB6/eGFP using ELAV-LG promoter. The anti-Htt antibody was used for detection of HttQ100-mRFP (100kDa = monomers , 70kDa = cleaved products,, 130-170kDa = intermediate aggregated species, stacking gel = HMW aggregates). The anti-V5 antibody was used for V5-DNAJB6b detection and Tubulin was used as loading control. Quantification of HttQ100-mRFP HMW aggregates normalized against tubulin shown for each line. Genotypes: 1) Control line (red): w(-); UAS HttQ100-mRFP / ELAV LG; ELAV Gal4 / LexO eGFP. 2) Rescued line (blue) w(-); UAS HttQ100-mRFP / ELAV LG; ELAV Gal4 / LexO DNAJB6.*

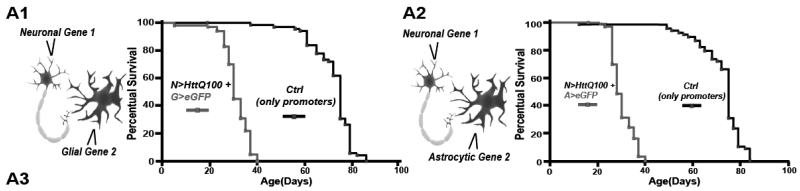

A3

NR	LINE	GENOTYPE	#DEATHS	MEDIAN SURVIVAL	COMPARISON	TEST 1	TEST 2
1	ELAV Gal4> +; REPO LhG>+	w(-); REPO LhG/+; ELAV Gal4/+	68	75			
2	ELAV Gal4> uas HTTQ100; REPO LhG>LexO eGFP	w(-); uas HttQ100/REPO LhG; ELAV Gal4/LexO eGFP	100	30	nr 2 vs nr 1	Significant,P<0,0001(***)	Significant,P<0,0001(***)
3	ELAV Gal4> uas HTTQ100; REPO LhG>LexO DNAJB6b	w(-); uas HttQ100/REPO LhG; ELAV Gal4/LexO DNAjb6b	95	37	nr 3 vs nr2	Significant,P<0,0001(***)	Significant,P<0,0001(***)
4	ELAV Gal4> +; ALRM LhG>+	w(-);ALRM LhG/+; ELAV Gal4/+	68	75			
5	ELAV Gal4> uas HTTQ100; ALRM LhG>LexO eGFP	w(-); uas HttQ100/ALRM LhG; ELAV Gal4/LexO eGFP	99	28	nr 5 vs nr 4	Significant,P<0,0001(***)	Significant,P<0,0001(***)
6	ELAV Gal4> uas HTTQ100; ALRM LhG>LexO DNAJB6b	w(-); uas HttQ100/ALRM LhG; ELAV Gal4/LexO DNAjb6b	104	35	nr 6 vs nr 5	Significant,P<0,0001(***)	Significant,P<0,0001(***)

TEST 1: LOG RANK (Mantel-Cox) Test
TEST 2: Gehan-Breslow-Wilcoxon Test

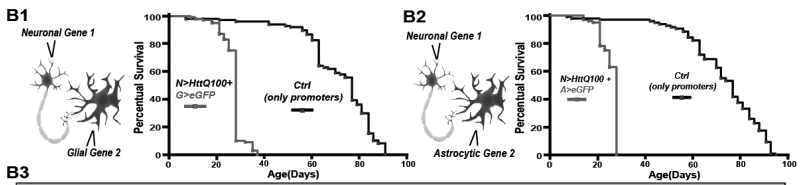

B3

NR	LINE	GENOTYPE	#DEATHS	MEDIAN SURVIVAL	COMPARISON	TEST 1	TEST 2
1	ELAV Gal4> +; REPO LG>+	w(-); REPO LG/+; ELAV Gal4/+	97	77			
2	ELAV Gal4> uas HTTQ100; REPO LG>LexO eGFP	w(-); uas HttQ100/REPO LG; ELAV Gal4/LexO eGFP	100	28	nr 2 vs nr 1	Significant,P<0,0001(***)	Significant,P<0,0001(***)
3	ELAV Gal4> uas HTTQ100; REPO LG>LexO DNAJB6b	w(-); uas HttQ100/REPO LG; ELAV Gal4/LexO DNAjb6b	78	28	nr 3 vs nr 2	Significant,P<0,0001(***)	**
4	ELAV Gal4> +; ALRM LG>+	w(-);ALRM LG/+; ELAV Gal4/+	96	77			
5	ELAV Gal4> uas HTTQ100; ALRM LG>LexO eGFP	w(-); uas HttQ100/ALRM LG; ELAV Gal4/LexO eGFP	100	28	nr 5 vs nr 4	Significant,P<0,0001(***)	Significant,P<0,0001(***)
6	ELAV Gal4> uas HTTQ100; ALRM LG>LexO DNAJB6b	w(-); uas HttQ100/ALRM LG; ELAV Gal4/LexO DNAjb6b	75	28	nr 6 vs nr 5	Significant,P<0,0001(***)	Significant,P=0,0005(***)

TEST 1: LOG RANK (Mantel-Cox) Test
TEST 2: Gehan-Breslow-Wilcoxon Test

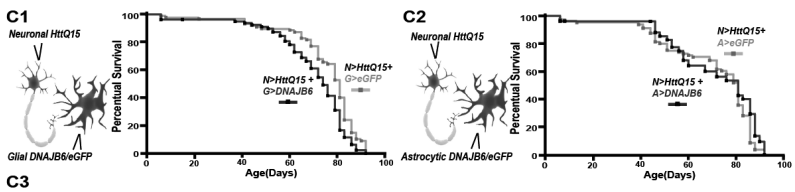

C3

NR	LINE	GENOTYPE	#DEATHS	MEDIAN SURVIVAL	COMPARISON	TEST 1	TEST 2
1	ELAV Gal4> uas HTTQ15; REPO LHg>LexO eGFP	w(-); uas Htt Q15/REPO LHg; ELAV Gal4/LexO eGFP	87	81			
2	ELAV Gal4> uas HTTQ15; REPO LHg>LexO DNAJB6b	w(-); uas Htt Q15/REPO LHg; ELAV Gal4/LexO DNAjb6b	77	74	nr 2 vs nr 1	Significant (**, p=0,0014)	Significant (**, p=0,0021)
3	ELAV Gal4> uas HTTQ15; ALRM LHg>LexO eGFP	w(-); uas Htt Q15/ALRM LHg; ELAV Gal4/LexO eGFP	81	81			
4	ELAV Gal4> uas HTTQ15; ALRM LHg>LexO DNAJB6b	w(-); uas Htt Q15/ALRM LHg; ELAV Gal4/LexO DNAjb6b	75	81	nr 4 vs nr 3	ns	ns

TEST 1: LOG RANK (Mantel-Cox) Test
TEST 2: Gehan-Breslow-Wilcoxon Test

Figure S4. A) *Lifespan of additional isogenized D. melanogaster control lines (♂,,S4A1, S4A2), statistics, and genotypes (S4A3) for experiment in Fig. 4D and 4F (LexO-DNAJB6/eGFP with LhG-strong expression). D. melanogaster co-expressing HttQ100-mRFP in neurons (N, via ELAV) and DNAJB6/eGFP in glial cells (G, via REPO, S4A1) or astrocytes (A, using ALRM, S4A2).* ***B)*** *Lifespan of additional isogenized D. melanogaster control lines (♂,S4B1, S4B2), statistics, and genotypes (S4B3) for experiment in Fig. 4C and 4E (LexO-DNAJB6/eGFP with LG-moderate expression). D. melanogaster co-expressing HttQ100-mRFP in neurons (N, via ELAV) and DNAJB6/eGFP in glial cells (G, via REPO, S4B1) or astrocytes (A, via ALRM, S4B2).* ***C)*** *Lifespan, statistics, and genotypes of isogenized D. melanogaster lines (♂) co-expressing HttQ15-mRFP in neurons (N, via ELAV) and DNAJB6/eGFP in glial cells (G, via REPO, S4C1) or astrocytes (A, via ALRM, S4C2). Strong expression of LexO-DNAJB6/eGFP was driven by the ELAV-LhG promoter. Statistical significance was analyzed in ≈100 flies/group by Log rank Mantel-Cox test.*

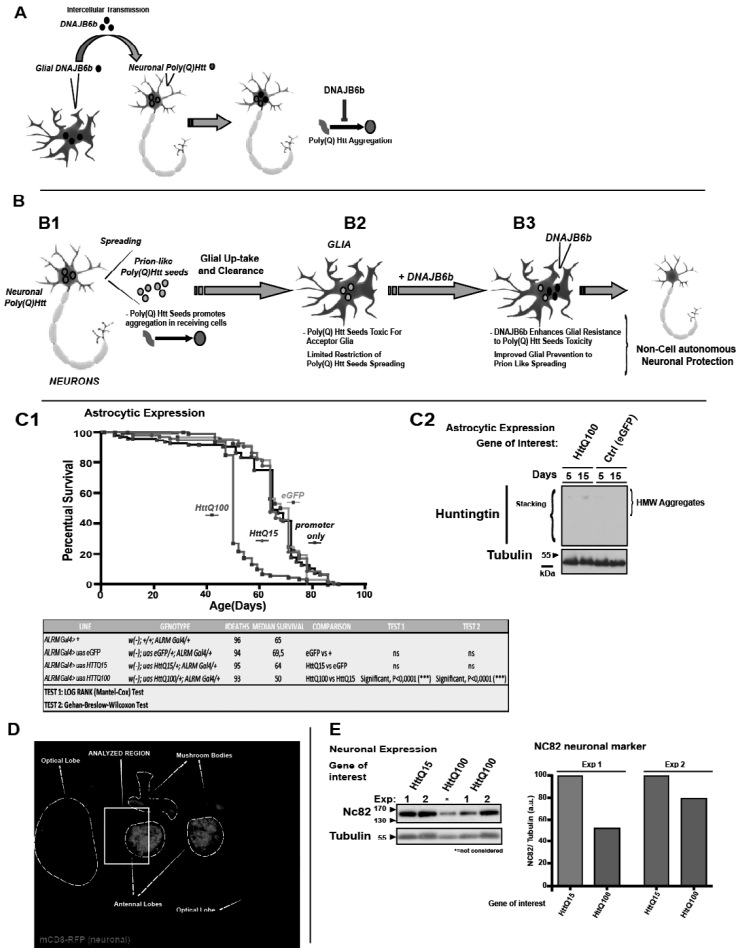

LINE	GENOTYPE	#DEATHS	MEDIAN SURVIVAL	COMPARISON	TEST1	TEST2
ALRM Gal4> +	w(-); +/+; ALRM Gal4/+	96	65			
ALRM Gal4> uas eGFP	w(-); uas eGFP/+; ALRM Gal4/+	94	60,5	eGFP vs +	ns	ns
ALRM Gal4> uas HTTQ15	w(-); uas HttQ15/+; ALRM Gal4/+	95	64	HttQ15 vs eGFP	ns	ns
ALRM Gal4> uas HTTQ100	w(-); uas HttQ100/+; ALRM Gal4/+	93	50	HttQ100 vs HttQ15	Significant, P<0,0001 (***)	Significant, P<0,0001 (***)
TEST 1: LOG RANK (Mantel-Cox) Test						
TEST 2: Gehan-Breslow-Wilcoxon Test						

Figure S5. A) *Possible intercellular DNAJB6 transmission from glial cells to neurons where the chaperone may lead to reduced aggregation of Poly(Q) Htt.* ***B)*** *Spreading of Poly(Q) Htt prion-like species (B1), role of glial cells in up-take and clearance of seeds (B2) and the non-cell autonomous protection of neurons through expression of DNAJB6 in glial cells (B3).* ***C)*** *Lifespan, statistics and genotypes (C1) of D. melanogaster lines (♂, Gal4-UAS system) expressing HttQ100-mRFP or control transgene (HttQ15-mRFP, eGFP or only promoter) in all astrocytes (using ALRM). Statistical significance analyzed using ≈100 flies/group with Log rank Mantel-Cox test.. Representative Western Blot of total heads lysates of indicated D. melanogaster lines is shown in C2. Anti-huntingtin antibody used for detection HMW aggregates (stacking gel) of HttQ100-mRFP. Tubulin as loading control.* ***D)*** *Representative confocal image of D. melanogaster brain (expressing pan-neuronal mCD8-RFP, via ELAV), showing the different neuronal lobes and highlighting the central brain region analyzed for data of Fig 5B and 5C.* ***E)*** *Representative Western Blots of total heads lysates of D. melanogaster lines (♀, 15 days old adults) expressing neuronal HttQ15-mRFP or HttQ100-mRFP (Gal4-UAS) using ELAV. Anti-NC82 antibody for NC82. Tubulin as loading control. Quantification of NC82 (signal normalized on tubulin signal) for each line and for each experiment at day 15 is shown. Genotypes: w(-); UAS HttQ15-mRFP (or UAS HttQ100-mRFP) / +; ELAV Gal4/+.*

Acknowledgments

We thank Jean Christophe Billeter for his significant contribution to the theoretical development of the *D. melanogaster* model, and Wondwossen Yeshaw and Serena Carra for their practical and intellectual contributions to the work underlying this manuscript.

Conflict of interest

HHK was involved in a regional initiative (SNN project Transitie II & Pieken) called ChaperoneAge, a consortium with commercial partners Syncom, ABL, Axon MedChem, Nyken, Brains-on-line, Angita Pharma, and the RuG/UMCG. HHK received research grants from Prinses Beatrix Spierfonds, the Hersenstichting, the High-Q foundation, the Ministry of Economic Affaires (senternoven.nl), and the National Ataxia Foundation. MMB was a graduate student at the University Medical Center Groningen at the time the study was conducted and is currently employed by PAREXEL International.

References

1. Kakkar, V., Meister-Broekema, M., Minoia, M., Carra, S. & Kampinga, H. H. Barcoding heat shock proteins to human diseases: looking beyond the heat shock response. *Dis. Model. Mech.* **7,** 421–434 (2014).
2. Sofroniew, M. V. & Vinters, H. V. Astrocytes: Biology and pathology. *Acta Neuropathol. (Berl.)* **119,** 7–35 (2010).
3. Hageman, J. *et al.* A DNAJB Chaperone Subfamily with HDAC-Dependent Activities Suppresses Toxic Protein Aggregation. *Mol. Cell* **37,** 355–369 (2010).
4. Kakkar, V. *et al.* The S/T-Rich Motif in the DNAJB6 Chaperone Delays Polyglutamine Aggregation and the Onset of Disease in a Mouse Model. *Mol. Cell* **62,** 272–283 (2016).
5. Weiss, K. R., Kimura, Y., Lee, W. C. M. & Littleton, J. T. Huntingtin aggregation kinetics and their pathological role in a drosophila Huntington's disease model. *Genetics* **190,** 581–600 (2012).
6. Hanai, R. & Mashima, K. Characterization of two isoforms of a human DnaJ homologue, HSJ2. *Mol. Biol. Rep.* **30,** 149–153 (2003).
7. Burr, A. A., Tsou, W. L., Ristic, G. & Todi, S. V. Using membrane-targeted green fluorescent protein to monitor neurotoxic protein-dependent degeneration of Drosophila eyes. *J. Neurosci. Res.* **92,** 1100–1109 (2014).
8. Brand, A. H. & Perrimon, N. Targeted gene expression as a means of altering cell fates and generating dominant phenotypes. *Dev. Camb. Engl.* **118,** 401–15 (1993).
9. Yao, K. M., Samson, M. L., Reeves, R. & White, K. Gene elav of Drosophila melanogaster: A prototype for neuronal-specific RNA binding protein gene family that is conserved in flies and humans. *J. Neurobiol.* **24,** 723–739 (1993).
10. Yagi, R., Mayer, F. & Basler, K. Refined LexA transactivators and their use in combination with the Drosophila Gal4 system. *Proc. Natl. Acad. Sci. U. S. A.* **107,** 16166–16171 (2010).
11. Månsson, C. *et al.* DNAJB6 is a peptide-binding chaperone which can suppress amyloid fibrillation of polyglutamine peptides at substoichiometric molar ratios. *Cell Stress Chaperones* **19,** 227–239 (2014).
12. Haim, L. B. & Rowitch, D. H. Functional diversity of astrocytes in neural circuit regulation. *Nat. Rev. Neurosci.* **18,** 31–41 (2017).
13. Sofroniew, M. V. Astrocyte barriers to neurotoxic inflammation. *Nat. Rev. Neurosci.* **16,** 249–263 (2015).
14. Ben Haim, L., Carrillo-de Sauvage, M.-A., Ceyzériat, K. & Escartin, C. Elusive roles for reactive astrocytes in neurodegenerative diseases. *Front. Cell. Neurosci.* **9,** 278 (2015).
15. Khakh, B. S. & Sofroniew, M. V. Astrocytes and Huntington's disease. *ACS Chem. Neurosci.* **5,** 494–496 (2014).
16. Doherty, J., Logan, M. A., Taşdemir, O. E. & Freeman, M. R. Ensheathing glia function as phagocytes in the adult Drosophila brain. *J. Neurosci. Off. J. Soc. Neurosci.* **29,** 4768–81 (2009).
17. Xiong, W.-C., Hideyuki, O., Patel, N. H., Blendy, J. A. & Montell, C. repo encodes a glial-specific homeo domain protein required in the Drosophila nervous system. *Genes Dev.* 981–994 (1994).
18. Takeuchi, T. *et al.* Intercellular chaperone transmission via exosomes contributes to maintenance of protein homeostasis at the organismal level. *Proc. Natl. Acad. Sci. U. S. A.* **112,** E2497-506 (2015).
19. Brundin, P., Melki, R. & Kopito, R. Prion-like transmission of protein aggregates in neurodegenerative diseases. *Nat. Rev. Mol. Cell Biol.* **11,** 301–7 (2010).
20. Costanzo, M. & Zurzolo, C. The cell biology of prion-like spread of protein aggregates: mechanisms and implication in neurodegeneration. *Biochem. J.* **452,** 1–17 (2013).
21. Ren, P.-H. *et al.* Cytoplasmic penetration and persistent infection of mammalian cells by polyglutamine aggregates. *Nat. Cell Biol.* **11,** 219–225 (2009).

22. Babcock, D. T. & Ganetzky, B. Transcellular spreading of huntingtin aggregates in the Drosophila brain. *Proc. Natl. Acad. Sci. U. S. A.* **112,** E5427-33 (2015).
23. Pearce, M. M. P., Spartz, E. J., Hong, W., Luo, L. & Kopito, R. R. Prion-like transmission of neuronal huntingtin aggregates to phagocytic glia in the Drosophila brain. *Nat. Commun.* **6,** 6768 (2015).
24. Wagh, D. A. *et al.* Bruchpilot, a protein with homology to ELKS/CAST, is required for structural integrity and function of synaptic active zones in Drosophila. *Neuron* **49,** 833–844 (2006).